

## 3-Space In-Flow Theory of Gravity: Boreholes, Blackholes and the Fine Structure Constant

Reginald T. Cahill

*School of Chemistry, Physics and Earth Sciences, Flinders University, Adelaide 5001, Australia*

E-mail: Reg.Cahill@flinders.edu.au

A theory of 3-space explains the phenomenon of gravity as arising from the time-dependence and inhomogeneity of the differential flow of this 3-space. The emergent theory of gravity has two gravitational constants:  $G_N$  — Newton's constant, and a dimensionless constant  $\alpha$ . Various experiments and astronomical observations have shown that  $\alpha$  is the fine structure constant  $\approx 1/137$ . Here we analyse the Greenland Ice Shelf and Nevada Test Site borehole  $g$  anomalies, and confirm with increased precision this value of  $\alpha$ . This and other successful tests of this theory of gravity, including the supermassive black holes in globular clusters and galaxies, and the “dark-matter” effect in spiral galaxies, shows the validity of this theory of gravity. This success implies that the non-relativistic Newtonian gravity was fundamentally flawed from the beginning, and that this flaw was inherited by the relativistic General Relativity theory of gravity.

### 1 Introduction

In the Newtonian theory of gravity [1] the Newtonian gravitational constant  $G_N$  determining the strength of this phenomenon is difficult to measure because of the extreme weakness of gravity. Originally determined in laboratory experiments by Cavendish [2] in 1798 using a torsion balance, Airy [3] in 1865 presented a different method which compared the gravity gradients above and below the surface of the Earth. Then if the matter density within the neighbourhood of the measurements is sufficiently uniform, or at most is horizontally layered and known, then such measurements then permitted  $G_N$  to be determined, as discussed below, if Newtonian gravity was indeed correct. Then the mass of the Earth can be computed from the value of  $g$  at the Earth's surface. However two anomalies have emerged for these two methods: (i) the Airy method has given gravity gradients that are inconsistent with Newtonian gravity, and (ii) the laboratory measurements of  $G_N$  using various geometries for the test masses have not converged despite ever increasing experimental sophistication and precision. There are other anomalies involving gravity such as the so-called “dark-matter” effect in spiral galaxies, the systematic effects related to the supermassive blackholes in globular clusters and elliptical galaxies, the Pioneer 10/11 deceleration anomaly, the so-called galactic ‘dark-matter’ networks, and others, all suggest that the phenomenon of gravity has not been understood even in the non-relativistic regime, and that a significant dynamical process has been overlooked in the Newtonian theory of gravity, and which is also missing from General Relativity.

The discovery of this missing dynamical process arose from experimental evidence [4, 8, 9] that a complex dynamical 3-space underlies reality. The evidence involves the

repeated detection of the motion of the Earth relative to that 3-space using Michelson interferometers operating in gas mode [8], particularly the experiment by Miller in 1925/26 at Mt. Wilson, and the coaxial cable RF travel time measurements by Torr and Kolen in Utah in 1985, and the DeWitte experiment in 1991 in Brussels [8]. In all 7 such experiments are consistent with respect to speed and direction. It has been shown that effects caused by motion relative to this 3-space can mimic the formalism of spacetime, but that it is the 3-space that is “real”, simply because it is directly observable [4].

The 3-space is in differential motion, that is one part has a velocity relative to other parts, and so involves a velocity field  $\mathbf{v}(\mathbf{r}, t)$  description. To be specific this velocity field must be described relative to a frame of observers, but the formalism is such that the dynamical equations for this velocity field must transform covariantly under a change of observer. It has been shown [4, 6] that the phenomenon of gravity is a consequence of the time-dependence and inhomogeneities of  $\mathbf{v}(\mathbf{r}, t)$ . So the dynamical equations for  $\mathbf{v}(\mathbf{r}, t)$  give rise to a new theory of gravity when combined with the generalised Schrödinger equation, and the generalised Maxwell and Dirac equations [10]. The equations for  $\mathbf{v}(\mathbf{r}, t)$  involve the gravitational constant\*  $G$  and a dimensionless constant that determines the strength of a new 3-space self-interaction effect, which is missing from both Newtonian Gravity and General Relativity. Experimental data has revealed [4, 5, 6] the remarkable discovery that this constant is the fine structure constant  $\alpha \approx e^2/\hbar c \approx 1/137$ . This dynamics then explains numerous gravitational anomalies, such as the borehole  $g$  anomaly, the so-called “dark matter” anomaly in the rotation speeds of spiral galaxies, and that the effective

\*This is different from the Newtonian effective gravitational constant  $G_N$  defined later.

mass of the necessary black holes at the centre of spherical matter systems, such as globular clusters and spherical galaxies, is  $\alpha/2$  times the total mass of these systems. This prediction has been confirmed by astronomical observations [7].

Here we analyse the Greenland and Nevada Test Site borehole  $g$  anomalies, and confirm with increased precision this value of  $\alpha$ .

The occurrence of  $\alpha$  suggests that space is itself a quantum system undergoing on-going classicalisation. Just such a proposal has arisen in *Process Physics* [4] which is an information-theoretic modelling of reality. There quantum space and matter arise in terms of the Quantum Homotopic Field Theory (QHFT) which, in turn, may be related to the standard model of matter. In the QHFT space at this quantum level is best described as a “quantum foam”. So we interpret the observed fractal\* 3-space as a classical approximation to this “quantum foam” [10].

## 2 Dynamical 3-space

Relative to some observer 3-space is described by a velocity field  $\mathbf{v}(\mathbf{r}, t)$ . It is important to note that the coordinate  $\mathbf{r}$  is not itself 3-space, rather it is merely a label for an element of 3-space that has velocity  $\mathbf{v}$ , relative to some observer. Also it is important to appreciate that this “moving” 3-space is not itself embedded in a “space”; the 3-space is all there is, although as noted above its deeper structure is that of a “quantum foam”.

In the case of zero vorticity  $\nabla \times \mathbf{v} = \mathbf{0}$  the 3-space dynamics is given by [4, 6], in the non-relativistic limit,

$$\nabla \cdot \left( \frac{\partial \mathbf{v}}{\partial t} + (\mathbf{v} \cdot \nabla) \mathbf{v} \right) + \frac{\alpha}{8} ((\text{tr} D)^2 - \text{tr}(D^2)) = -4\pi G \rho, \quad (1)$$

where  $\rho$  is the matter density, and where

$$D_{ij} = \frac{1}{2} \left( \frac{\partial v_i}{\partial x_j} + \frac{\partial v_j}{\partial x_i} \right). \quad (2)$$

The acceleration of an element of space is given by the Euler form

$$\mathbf{g}(\mathbf{r}, t) \equiv \lim_{\Delta t \rightarrow 0} \frac{\mathbf{v}(\mathbf{r} + \mathbf{v}(\mathbf{r}, t)\Delta t, t + \Delta t) - \mathbf{v}(\mathbf{r}, t)}{\Delta t} = \frac{\partial \mathbf{v}}{\partial t} + (\mathbf{v} \cdot \nabla) \mathbf{v}. \quad (3)$$

It was shown in [10] that matter has the same acceleration<sup>†</sup> as (3), which gave a derivation of the equivalence principle as a quantum effect in the Schrödinger equation when uniquely generalised to include the interaction of the quantum system with the 3-space. These forms are mandated by Galilean covariance under change of observer<sup>‡</sup>. This minimalist non-relativistic modelling of the dynamics for the velocity field

\*The fractal property of 3-space was found [10] from the DeWitte data.

<sup>†</sup>Except for the acceleration component induced by vorticity.

<sup>‡</sup>However this does not exclude so-called relativistic effects, such as the length contraction of moving rods or the time dilations of moving clocks.

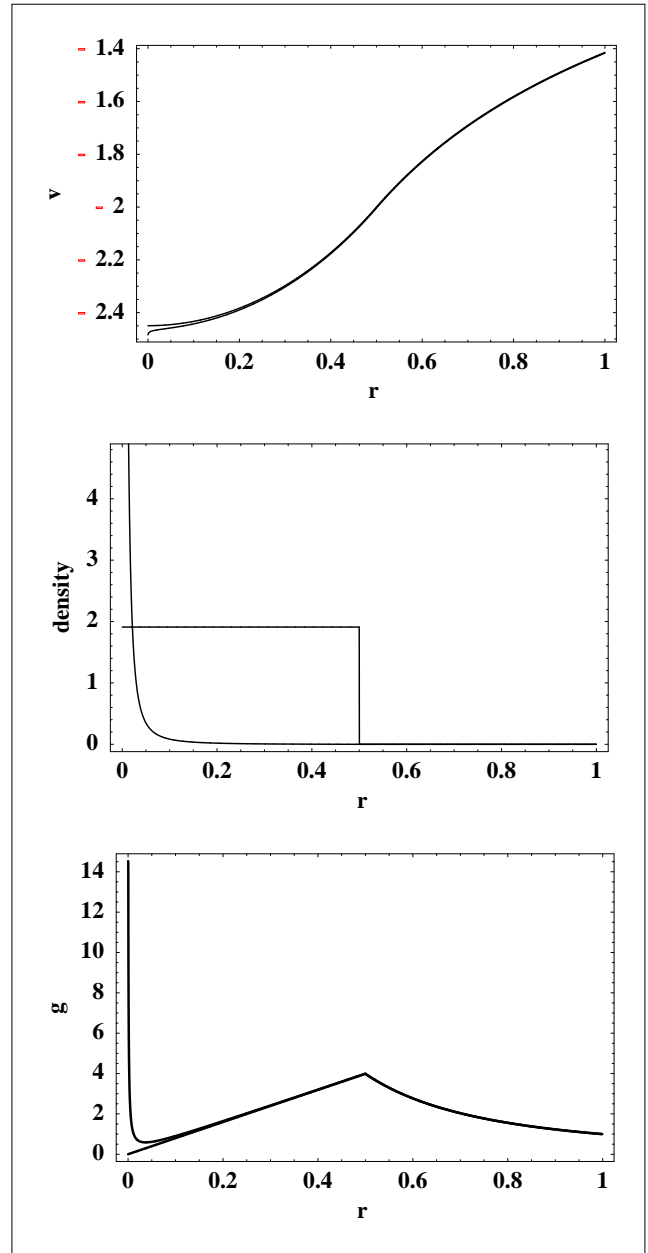


Fig. 1: Upper plot shows speeds from numerical iterative solution of (7) for a solid sphere with uniform density and radius  $r=0.5$  for (i) upper curve the case  $\alpha=0$  corresponding to Newtonian gravity, and (ii) lower curve with  $\alpha=1/137$ . These solutions only differ significantly near  $r=0$ . Middle plot shows matter density and “dark matter” density  $\rho_{DM}$ , from (5), with arbitrary scales. Lower plot shows the acceleration from (3) for (i) the Newtonian in-flow from the upper plot, and (ii) from the  $\alpha=1/137$  case. The difference is only significant near  $r=0$ . The accelerations begin to differ just inside the surface of the sphere at  $r=0.5$ , according to (15). This difference is the origin of the borehole  $g$  anomaly, and permits the determination of the value of  $\alpha$  from observational data. This generic singular- $g$  behaviour, at  $r=0$ , is seen in the Earth, in globular clusters and in galaxies.

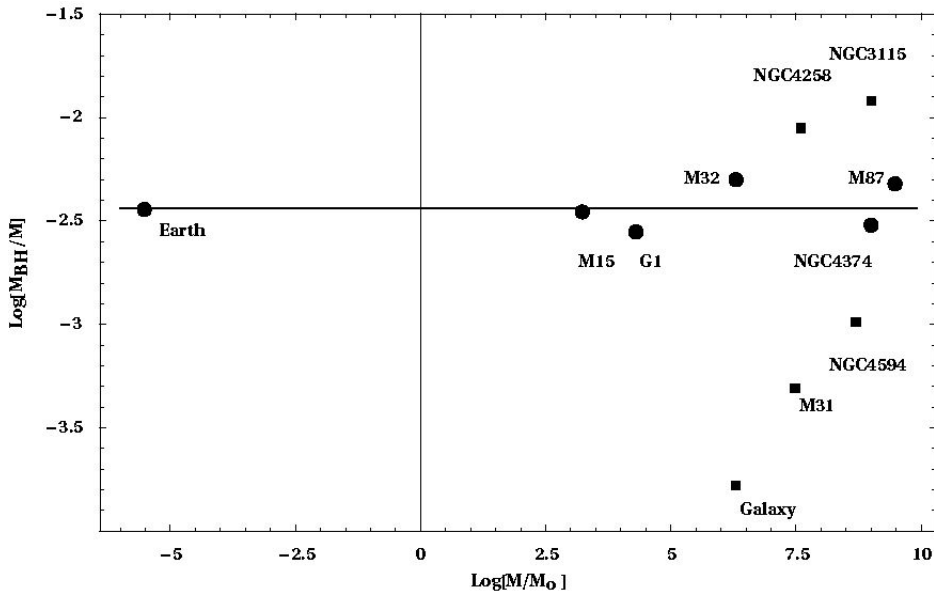


Fig. 2: The data shows  $\text{Log}_{10}[M_{BH}/M]$  for the “blackhole” or “dark matter” masses  $M_{BH}$  for a variety of spherical matter systems with masses  $M$ , shown by solid circles, plotted against  $\text{Log}_{10}[M/M_0]$ , where  $M_0$  is the solar mass, showing agreement with the “ $\alpha/2$ -line” ( $\text{Log}_{10}[\alpha/2] = -2.44$ ) predicted by (10), and ranging over 15 orders of magnitude. The “blackhole” effect is the same phenomenon as the “dark matter” effect. The data ranges from the Earth, as observed by the bore hole  $g$  anomaly, to globular cluster M15 and G1, and then to spherical “elliptical” galaxies M32 (E2), NGC 4374 (E1) and M87 (E0). Best fit to the data from these star systems gives  $\alpha = 1/134$ , while for the Earth data in Figs.3,4,5 give  $\alpha = 1/137$ . In these systems the “dark matter” or “black hole” spatial self-interaction effect is induced by the matter. For the spiral galaxies, shown by the filled boxes, where here  $M$  is the bulge mass, the blackhole masses do not correlate with the “ $\alpha/2$ -line”. This is because these systems form by matter in-falling to a primordial blackhole, and so these systems are more contingent. For spiral galaxies this dynamical effect manifests most clearly via the non-Keplerian rotation-velocity curve, which decrease asymptotically very slowly. See [7] for references to the data.

gives a direct account of the various phenomena noted above. A generalisation to include relativistic effects of the motion of matter through this 3-space is given in [4]. From (1) and (3) we obtain that

$$\nabla \cdot \mathbf{g} = -4\pi G\rho - 4\pi G\rho_{DM}, \quad (4)$$

where

$$\rho_{DM}(\mathbf{r}) = \frac{\alpha}{32\pi G} ((\text{tr}D)^2 - \text{tr}(D^2)). \quad (5)$$

In this form we see that if  $\alpha \rightarrow 0$ , then the acceleration of the 3-space elements is given by Newton’s *Universal Law of Gravitation*, in differential form. But for a non-zero  $\alpha$  we see that the 3-space acceleration has an additional effect, from the  $\rho_{DM}$  term, which is an effective “matter density” that mimics the new self-interaction dynamics. This has been shown to be the origin of the so-called “dark matter” effect in spiral galaxies. It is important to note that (4) does not determine  $\mathbf{g}$  directly; rather the velocity dynamics in (1) must be solved, and then with  $\mathbf{g}$  subsequently determined from (3). Eqn.(4) merely indicates that the resultant non-Newtonian  $\mathbf{g}$  could be mistaken as the result of a new form of matter, whose density is given by  $\rho_{DM}$ . Of course the saga of “dark matter” shows that this actually happened, and

that there has been a misguided and fruitless search for such “matter”.

### 3 Airy method for determining $\alpha$

We now show that the Airy method actually gives a technique for determining the value of  $\alpha$  from Earth based borehole gravity measurements. For a time-independent velocity field (1) may be written in the integral form

$$|\mathbf{v}(\mathbf{r})|^2 = 2G \int d^3r' \frac{\rho(\mathbf{r}') + \rho_{DM}(\mathbf{r}')}{|\mathbf{r} - \mathbf{r}'|}. \quad (6)$$

When the matter density of the Earth is assumed to be spherically symmetric, and that the velocity field is now radial\* (6) becomes

$$v(r)^2 = \frac{8\pi G}{r} \int_0^r s^2 [\rho(s) + \rho_{DM}(s)] ds + 8\pi G \int_r^\infty s [\rho(s) + \rho_{DM}(s)] ds, \quad (7)$$

\*This in-flow is additional to the observed velocity of the Earth through 3-space.

where, with  $v' = dv(r)/dr$ ,

$$\rho_{DM}(r) = \frac{\alpha}{32\pi G} \left( \frac{v^2}{2r^2} + \frac{vv'}{r} \right). \quad (8)$$

Iterating (7) once we find to 1st order in  $\alpha$  that

$$\rho_{DM}(r) = \frac{\alpha}{2r^2} \int_r^\infty s\rho(s) ds + O(\alpha^2), \quad (9)$$

so that in spherical systems the “dark matter” effect is concentrated near the centre, and we find that the total “dark matter” is

$$\begin{aligned} M_{DM} &\equiv 4\pi \int_0^\infty r^2 \rho_{DM}(r) dr = \\ &= \frac{4\pi\alpha}{2} \int_0^\infty r^2 \rho(r) dr + O(\alpha^2) = \frac{\alpha}{2} M + O(\alpha^2), \end{aligned} \quad (10)$$

where  $M$  is the total amount of (actual) matter. Hence to  $O(\alpha)$   $M_{DM}/M = \alpha/2$  independently of the matter density profile. This turns out to be a very useful property as complete knowledge of the density profile is then not required in order to analyse observational data. As seen in Fig. 1 the singular behaviour of both  $v$  and  $g$  means that there is a *blackhole\** singularity at  $r=0$ . Interpreting  $M_{DM}$  in (10) as the mass of the blackholes observed in the globular clusters M15 and G1 and in the highly spherical “elliptical” galaxies M32, M87 and NGC 4374, we obtained [7]  $\alpha \approx 1/134$ , as shown in Fig. 2.

From (3), which is also the acceleration of matter [10], the gravity acceleration<sup>†</sup> is found to be, to 1st order in  $\alpha$ , and using that  $\rho(r)=0$  for  $r>R$ , where  $R$  is the radius of the Earth,

$$g(r) = \begin{cases} \frac{(1 + \frac{\alpha}{2}) GM}{r^2}, & r > R; \\ \frac{4\pi G}{r^2} \int_0^r s^2 \rho(s) ds + \\ + \frac{2\pi\alpha G}{r^2} \int_0^r \left( \int_s^R s' \rho(s') ds' \right) ds, & r < R. \end{cases} \quad (11)$$

This gives Newton’s “inverse square law” for  $r>R$ , even when  $\alpha \neq 0$ , which explains why the 3-space self-interaction dynamics did not overtly manifest in the analysis of planetary orbits by Kepler and then Newton. However inside the Earth (11) shows that  $g(r)$  differs from the Newtonian theory, corresponding to  $\alpha=0$ , as Fig. 1, and it is this effect that allows the determination of the value of  $\alpha$  from the Airy method.

Expanding (11) in  $r$  about the surface,  $r=R$ , we obtain, to 1st order in  $\alpha$  and for an arbitrary density profile,

\*These are called *blackholes* because there is an event horizon, but in all other aspects differ from the *blackholes* of General Relativity.

†We now use the convention that  $g(r)$  is positive if it is radially inward.

$$g(r) = \begin{cases} \frac{G_N M}{R^2} - \frac{2G_N M}{R^3}(r-R), & r > R; \\ \frac{G_N M}{R^2} - \left( \frac{2G_N M}{R^3} - 4\pi \left(1 - \frac{\alpha}{2}\right) G_N \rho \right) \times \\ \times (r-R), & r < R. \end{cases} \quad (12)$$

where  $\rho$  is the matter density at the surface,  $M$  is the total matter mass of the Earth, and where we have defined

$$G_N \equiv \left(1 + \frac{\alpha}{2}\right) G. \quad (13)$$

The corresponding Newtonian gravity expression is obtained by taking the limit  $\alpha \rightarrow 0$ ,

$$g_N(r) = \begin{cases} \frac{G_N M}{R^2} - \frac{2G_N M}{R^3}(r-R), & r > R; \\ \frac{G_N M}{R^2} - \left( \frac{2G_N M}{R^3} - 4\pi G_N \rho \right) (r-R), & r < R. \end{cases} \quad (14)$$

Assuming Newtonian gravity (14) then means that from the measurement of difference between the above-ground and below-ground gravity gradients, namely  $4\pi G_N \rho$ , and also measurement of the matter density, permit the determination of  $G_N$ . This is the basis of the Airy method for determining  $G_N$  [3].

When analysing the borehole data it has been found [11, 12] that the observed difference of the density gradients was inconsistent with  $4\pi G_N \rho$  in (14), in that it was not given by the laboratory value of  $G_N$  and the matter density. This is known as the borehole  $g$  anomaly and which attracted much interest in the 1980’s. The key point in understanding this anomaly is that even allowing for the dynamical rescaling of  $G$ , expressions (12) and (14) have a different dependence on  $r-R$  beneath the surface. The borehole data papers [11, 12] report the discrepancy, i.e. the anomaly or the gravity residual as it is called, between the Newtonian prediction and the measured below-earth gravity gradient. Taking the difference between (12) and (14), assuming the same unknown value of  $G_N$  in both, we obtain an expression for the gravity residual

$$\Delta g(r) \equiv g_N(r) - g(r) = \begin{cases} 0, & r > R; \\ 2\pi\alpha G_N \rho (r-R), & r < R. \end{cases} \quad (15)$$

When  $\alpha \neq 0$  we have a two-parameter theory of gravity, and from (11) we see that measurement of the difference between the above ground and below ground gravity gradients is  $4\pi \left(1 - \frac{\alpha}{2}\right) G_N \rho$ , and this is not sufficient to determine both  $G_N$  and  $\alpha$ , given  $\rho$ , and so the Airy method is now understood not to be a complete measurement by itself, i.e. we need to combine it with other measurements. If we now use laboratory Cavendish experiments to determine  $G_N$ , then from the borehole gravity residuals we can determine the value of  $\alpha$ , as already indicated in [5, 6]. As discussed in Sect. 7 these Cavendish experiments can only determine  $G_N$

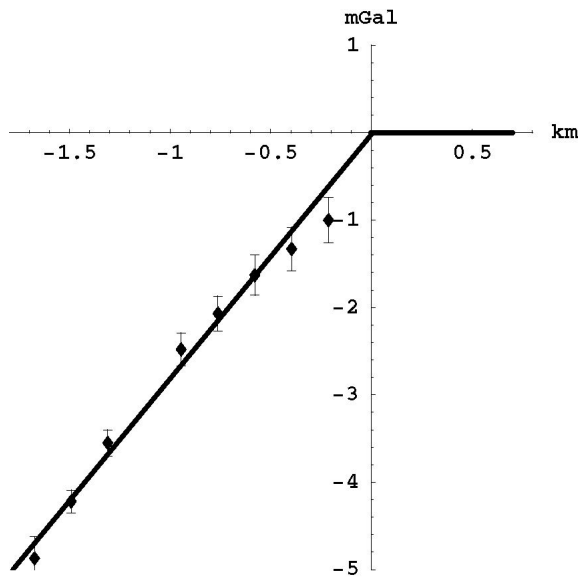


Fig. 3: The data shows the gravity residuals for the Greenland Ice Shelf [11] Airy measurements of the  $g(r)$  profile, defined as  $\Delta g(r) = g_{\text{Newton}} - g_{\text{observed}}$ , and measured in mGal ( $1\text{mGal} = 10^{-3} \text{ cm/s}^2$ ) and plotted against depth in km. The gravity residuals have been offset. The borehole effect is that Newtonian gravity and the new theory differ only beneath the surface, provided that the measured above surface gravity gradient is used in both theories. This then gives the horizontal line above the surface. Using (15) we obtain  $\alpha^{-1} = 137.9 \pm 5$  from fitting the slope of the data, as shown. The non-linearity in the data arises from modelling corrections for the gravity effects of the irregular sub ice-shelf rock topography.

up to corrections of order  $\alpha/4$ , simply because the analysis of the data from these experiments assumed the validity of Newtonian gravity. So the analysis of the borehole residuals will give the value of  $\alpha$  up to  $O(\alpha^2)$  corrections, which is consistent with the  $O(\alpha)$  analysis reported above.

#### 4 Greenland Ice Shelf borehole data

Gravity residuals from a bore hole into the Greenland Ice Shelf were determined down to a depth of 1.5 km by Ander *et al.* [11] in 1989. The observations were made at the Dye 3 2033 m deep borehole, which reached the basement rock. This borehole is 60 km south of the Arctic Circle and 125 km inland from the Greenland east coast at an elevation of 2530 m. It was believed that the ice provided an opportunity to use the Airy method to determine  $G_N$ , but now it is understood that in fact the borehole residuals permit the determination of  $\alpha$ , given a laboratory value for  $G_N$ . Various steps were taken to remove unwanted effects, such as imperfect knowledge of the ice density and, most dominantly, the terrain effects which arises from ignorance of the profile and density inhomogeneities of the underlying rock. The

borehole gravity meter was calibrated by comparison with an absolute gravity meter. The ice density depends on pressure, temperature and air content, with the density rising to its average value of  $\rho = 920 \text{ kg/m}^3$  within some 200 m of the surface, due to compression of the trapped air bubbles. This surface gradient in the density has been modelled by the author, and is not large enough to affect the results. The leading source of uncertainty was from the gravitational effect of the bedrock topography, and this was corrected for using Newtonian gravity. The correction from this is actually the cause of the non-linearity of the data points in Fig. 3. A complete analysis would require that the effect of this rock terrain be also computed using the new theory of gravity, but this was not done. Using  $G_N = 6.6742 \times 10^{-11} \text{ m}^3\text{s}^{-2}\text{kg}^{-1}$ , which is the current CODATA value, see Sect. 7, we obtain from a least-squares fit of the linear term in (15) to the data points in Fig. 3 that  $\alpha^{-1} = 137.9 \pm 5$ , which equals the value of the fine structure constant  $\alpha^{-1} = 137.036$  to within the errors, and for this reason we identify the constant  $\alpha$  in (1) as being the fine structure constant. The first analysis [5, 6] of the Greenland Ice Shelf data incorrectly assumed that the ice density was  $930 \text{ kg/m}^3$  which gave  $\alpha^{-1} = 139 \pm 5$ . However trapped air reduces the standard ice density to the ice shelf density of  $920 \text{ kg/m}^3$ , which brings the value of  $\alpha$  immediately into better agreement with the value of  $\alpha = e^2/\hbar c$  known from quantum theory.

#### 5 Nevada Test Site borehole data

Thomas and Vogel [12] performed another borehole experiment at the Nevada Test Site in 1989 in which they measured the gravity gradient as a function of depth, the local average matter density, and the above ground gradient, also known as the free-air gradient. Their intention was to test the extracted  $G_{\text{local}}$  and compare with other values of  $G_N$ , but of course using the Newtonian theory. The Nevada boreholes, with typically 3 m diameter, were drilled as a part of the U.S. Government tests of its nuclear weapons. The density of the rock is measured with a  $\gamma - \gamma$  logging tool, which is essentially a  $\gamma$ -ray attenuation measurement, while in some holes the rock density was measured with a coring tool. The rock density was found to be  $2000 \text{ kg/m}^3$ , and is dry. This is the density used in the analysis herein. The topography for 1 to 2 km beneath the surface is dominated by a series of overlapping horizontal lava flows and alluvial layers. Gravity residuals from three of the bore holes are shown in Figs. 4, 5 and 6. All gravity measurements were corrected for the Earth's tide, the terrain on the surface out to 168 km distance, and the evacuation of the holes. The gravity residuals arise after allowing for, using Newtonian theory, the local lateral mass anomalies but assumed that the matter beneath the holes occurs in homogeneous ellipsoidal layers. Here we now report a detailed analysis of the Nevada data. First we note that the gravity residuals from borehole U20AO, Fig. 6,

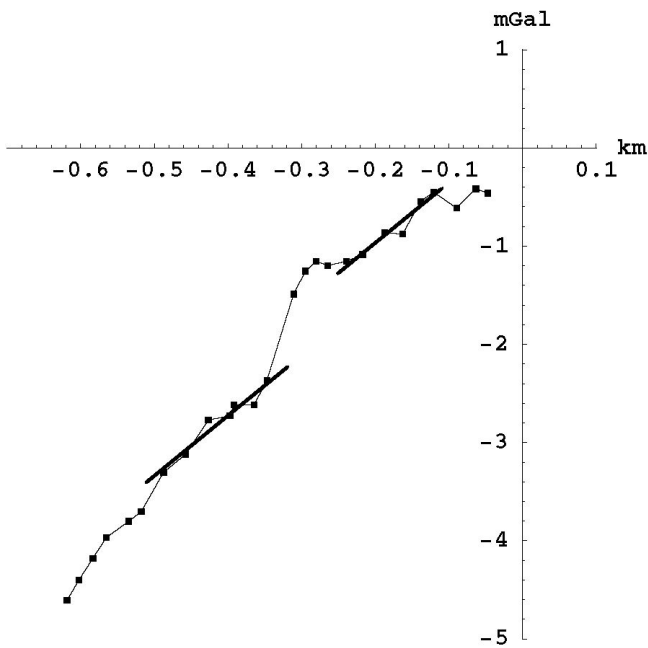


Fig. 4: The data shows the gravity residuals for the Nevada U20AK borehole Airy measurements of the  $g(r)$  profile [12], defined as  $\Delta g(r) = g_{\text{Newton}} - g_{\text{observed}}$ , and measured in mGal, plotted against depth in km. This residual shows regions of linearity interspersed with regions of non-linearity, presumably arising from layers with a density different from the main density of  $2000 \text{ kg/m}^3$ . Density changes generate a change in the (arbitrary) residual offset. From a least-squares simultaneous fit of the linear form in (15) to the four linear regions in this data and that in Fig. 5 for the data from borehole U20AL, we obtain  $\alpha^{-1} = 136.8 \pm 3$ . The two fitted regions of data are shown by the two straight lines here and in Fig. 5.

are not sufficiently linear to be useful. This presumably arises from density variations caused by the layering effect. For boreholes UA20AK, Fig. 4, and UA20AL, Fig. 5, we see segments where the gravity residuals are linear with depth, where the density is the average value of  $2000 \text{ kg/m}^3$ , but interspersed with layers where the residuals show non-linear changes with depth. It is assumed here that these non-linear regions are caused by variable density layers. So in analysing this data we have only used the linear regions, and a simultaneous least-squares fit to (15), with again  $G_N = 6.6742 \times 10^{-11} \text{ m}^3 \text{ s}^{-2} \text{ kg}^{-1}$  as for the Greenland data analysis, of these four linear regions gives  $\alpha^{-1} = 136.8 \pm 3$ , which again is in extraordinary agreement with the value of 137.04 from quantum theory.

## 6 Ocean measurements

The ideal Airy experiment would be one using the ocean, as all relevant physical aspects are accessible. Such an experiment was carried out by Zumberge *et al.* in 1991 [13]

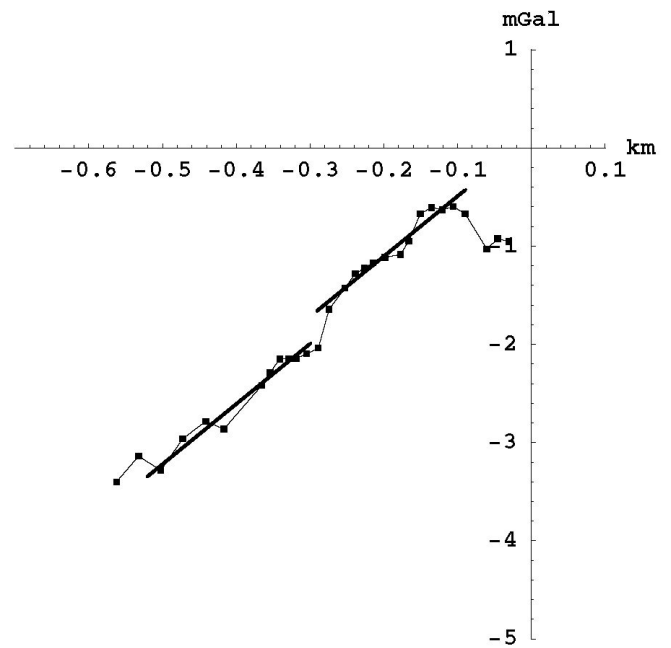


Fig. 5: The data shows the gravity residuals for the Nevada U20AL borehole Airy measurements of the  $g(r)$  profile [12], defined as  $\Delta g(r) = g_{\text{Newton}} - g_{\text{observed}}$ , and measured in mGal, plotted against depth in km. This residual shows regions of linearity interspersed with regions of non-linearity, presumably arising from layers with a density different from the main density of  $2000 \text{ kg/m}^3$ . Density changes generate a change in the (arbitrary) residual offset. From a least-squares simultaneous fit of the linear form in (15) to the four linear regions in this data and that in Fig. 4 for the data from borehole U20AK in Fig. 4, we obtain  $\alpha^{-1} = 136.8 \pm 3$ . The two fitted regions of data are shown by the two straight lines here and in Fig. 4.

using submersibles. Corrections for sea floor topography, seismic profiles and sea surface undulations were carried out. However a true Airy experiment appears not to have been performed. That would have required the measurement of the above and below sea-surface gravity gradients. Rather only the below sea-surface gradients were measured, and compared with a predicted gravity gradient using the density of the water and a laboratory value of  $G_N$  from only one such experiment and, as shown in Fig. 7, these have a large uncertainty. Hence this experiment does not permit an analysis of the data of the form applied to the Greenland and Nevada observations. The value of  $G_N$  from this ocean experiment is shown in Fig. 7 as experiment #12.

## 7 $G$ experiments

The new theory of gravity, given in (1) for the case of zero vorticity and in the non-relativistic limit, is a two-parameter theory;  $G$  and  $\alpha$ . Hence in experiments to determine  $G$  (or  $G_N$ ) we expect to see systematic discrepancies if the

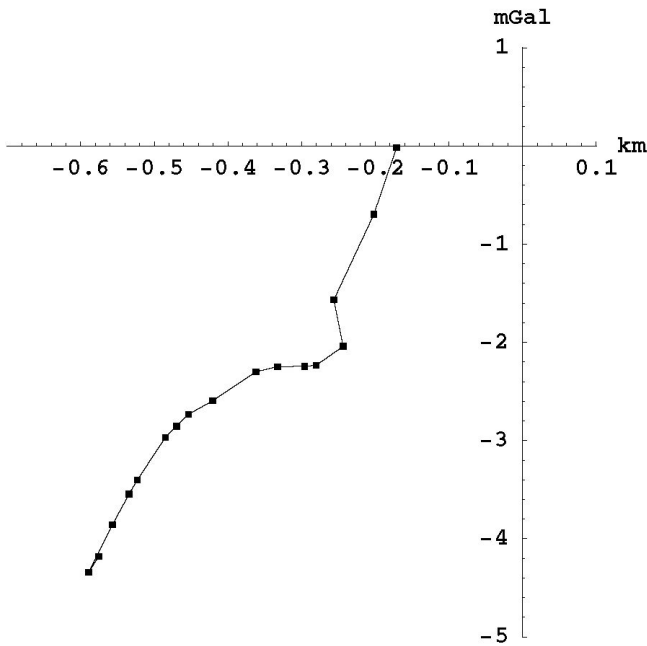


Fig. 6: The data shows the gravity residuals from the third Nevada U20AO borehole Airy measurements of the  $g(r)$  profile [12]. This data is not of sufficient linearity, presumably due to non-uniformity of density, to permit a fit to the linear form in (15), but is included here for completeness. There is an arbitrary offset in the residual.

Newtonian theory is used to analyse the data. This is clearly the case as shown in Fig. 7 which shows the results of such analyses over the last 60 years. The fundamental problem is that non-Newtonian effects of size  $\Delta G_N/G_N \approx \alpha/4$  are clearly evident, and effects of this size are expected from (1). To correctly analyse data from these experiments the full theory in (1) must be used, and this would involve (i) computing the velocity field for each configuration of the test masses, and then (ii) computing the forces by using (3) to compute the acceleration field. These computations are far from simple, especially when the complicated matter geometries of recent experiments need to be used. Essentially the flow of space results in a non-Newtonian effective “dark matter” density in (5). This results in deviations from Newtonian gravity which are of order  $\alpha/4$ . The prediction is that when laboratory Cavendish-type experiments are correctly analysed the data will permit the determination of both  $G_N$  and  $\alpha$ , and the large uncertainties in the determination of  $G_N$  will no longer occur. Until then the value of  $G_N$  will continue to be the least accurately known of all the fundamental constants. Despite this emerging insight CODATA\* in 2005 [20] reduced the apparent uncertainties in  $G_N$  by a factor of 10, and so ignoring the manifest presence of a systematic effect. The occurrence of the fine structure constant  $\alpha$ , in

\*CODATA is the Task Group on Fundamental Constants of the Committee on Data for Science and Technology, established in 1969.

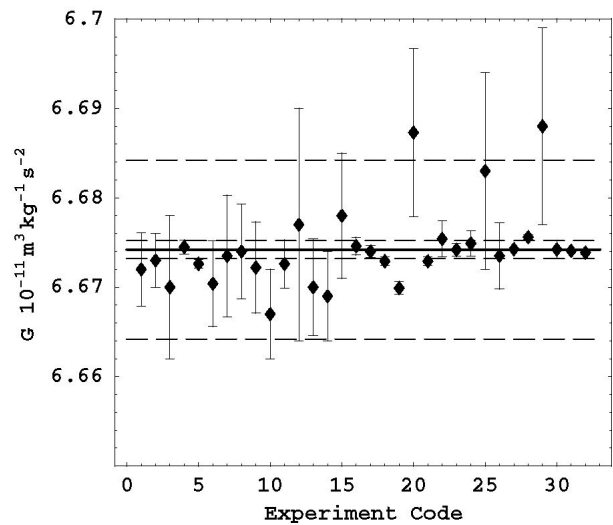


Fig. 7: Results of precision measurements of  $G_N$  published in the last sixty years in which the Newtonian theory was used to analyse the data. These results show the presence of a systematic effect, not in the Newtonian theory, of fractional size up to  $\Delta G_N/G_N \approx \alpha/4$ , which corresponded with the 1998 error bars on  $G_N$  (outer dashed lines), with the full line being the current CODATA value of  $G_N = 6.6742(10) \times 10^{-11} \text{ m}^2 \text{ s}^{-2} \text{ kg}^{-1}$ . In 2005 CODATA [20] reduced the error bars by a factor of 10 (inner dashed lines) on the basis of some recent experiments, and so neglecting the presence of the systematic effect.

giving the magnitude of the spatial self-interaction effect in (1), is a fundamental development in our understanding of 3-space and the phenomenon of gravity. Indeed the implication is that  $\alpha$  arises here as a manifestation of quantum processes inherent in 3-space.

### 8 Some history

Here we have simply applied the new two-parameter theory of 3-space, and hence of gravity, to the existing data from borehole experiments. However the history of these experiments shows that, of course, the nature of the gravitational anomaly had not been understood, and so the implications for fundamental physics that are now evident could not have been made. The first indications that some non-Newtonian effect was being observed arose from Yellin [14] and Hinze *et al.* [15]. It was Stacey *et al.* in 1981 [17, 16, 18] who undertook systematic studies at the Mt. Isa mine in Queensland, Australia. In the end a mine site is very unsuited for such a gravitational anomaly experiment as by their very nature mines have non-uniform poorly-known density and usually, as well, irregular surface topography. In the end it was acknowledged that the Mt. Isa mine data was unreliable. Nevertheless those reports motivated the Greenland, Nevada and Ocean experiments, as well as above-ground tower exper-

riments [19], all with the assumption that the non-Newtonian effects were being caused by a modification to Newton's *inverse square law* by an additional short-range force — which also involved the notion of a possible “5th-force” [21]. However these interpretations were not supported by the data, and eventually the whole phenomenon of these gravitational borehole anomalies was forgotten.

## 9 Conclusions

We have extended the results from an earlier analysis [5, 6] of the Greenland Ice Shelf borehole  $g$  anomaly data by correcting the density of ice from the assumed value to the actual value. This brought the extracted value of  $\alpha$  from approximately  $1/139$  to approximately  $1/137$ , and so into even closer agreement with the quantum theory value. As well the analysis was extended to the Nevada borehole anomaly data, again giving  $\alpha \approx 1/137$ . This is significant as the rock density is more than twice the ice density. As well we have included the previous results [7] from analysis of the blackhole masses in globular clusters and elliptical “spherical” galaxies, which gave  $\alpha \approx 1/134$ , but with larger uncertainty. So the conclusion that  $\alpha$  is actually the fine structure constant from quantum theory is now extremely strong. These results, together with the successful explanation for the so-called spiral galaxy “dark-matter” effect afforded by the new theory of gravity, implies that the Newtonian theory of gravity [1] is fundamentally flawed, even at the non-relativistic level, and that the disagreement with experiment and observation can be of fractional order  $\alpha$ , or in the case of spiral galaxies and blackholes, extremely large. This failure implies that General Relativity, which reduces to the Newtonian theory in the non-relativistic limit, must also be considered as flawed and disproven.

## References

1. Newton I. *Philosophiae Naturalis Principia Mathematica*. 1687.
2. Cavendish H. *Philosophical Transactions*. 1798.
3. Airy G.B. *Philos. Trans. R. Soc. London*, 1856, v. 146, 297; v. 146, 343.
4. Cahill R.T. *Process Physics: from information theory to quantum space and matter*. Nova Science Pub., NY, 2005.
5. Cahill R. T. Gravitation, the “dark matter” effect, and the fine structure constant. *Apeiron*, 2005, v. 12(2), 155–177.
6. Cahill R. T. “Dark matter” as a quantum foam in-flow effect. In *Trends in Dark Matter Research*, ed. by J. Val Blain, Nova Science Pub., NY., 2005, 96–140.
7. Cahill R. T. Black holes in elliptical and spiral galaxies and in globular clusters. *Progress in Physics*, 2005, v. 3, 51–56.
8. Cahill R. T. The Michelson and Morley 1887 experiment and the discovery of absolute motion. *Progress in Physics*, 2005, v. 3, 25–29; Cahill R. T. and Kitto K. *Apeiron*, 2003, v. 10(2), 104–117.
9. Cahill R. T. Absolute motion and gravitational effects. *Apeiron*, 2004, v. 11(1), 53–111.
10. Cahill R.T. Dynamical fractal 3-space and the generalised Schrödinger equation: Equivalence principle and vorticity effects. *Progress in Physics*, 2006, v. 1, 27–34.
11. Ander M.E. *et al.* Test of Newton's inverse-square law in the Greenland Ice Cap. *Phys. Rev. Lett.*, 1989, v. 62, 985–988.
12. Thomas J. and Vogel P. Testing the inverse-square law of gravity in boreholes at the Nevada Test Site. *Phys. Rev. Lett.*, 1990, v. 65, 1173–1176.
13. Zumberge M.A. *et al.* Submarine measurement of the Newtonian gravitational constant. *Phys. Rev. Lett.*, 1991, v. 67, 3051–3054.
14. Yellin M. J. ESSA Operational data report C & GSDR-2. U.S. Dept. Commerce, Washington, 1968.
15. Hinze W.J., Bradley J. W., and Brown A. R. *J. Geophys. Res.*, 1978, v. 83, 5864.
16. Stacey F.C. *et al.* Constraints on the planetary scale of the Newtonian gravitational constant from the gravity profile within a mine. *Phys. Rev. D*, 1981, v. 23, 1683–1692.
17. Stacey F.D. and Tuck G.J. Geophysical evidence for non-Newtonian gravity. *Nature*, 1981, v. 292, 16–22.
18. Holding S.C., Stacey F.D., and Tuck G.J. Gravity in mines — an investigation of Newton's law. *Phys. Rev. D*, 1986, v. 33, 3487–3494.
19. Thomas J. *et al.* Testing the inverse-square law of gravity on a 465-m tower. *Phys. Rev. Lett.*, 1989, v. 63, 1902–1905.
20. Mohr P.J. and Taylor B.N. CODATA recommended values of the fundamental physical constants: 2002. *Rev. Mod. Phys.*, 2005, v. 77(1), 1–107.
21. Fischbach E. and Talmadge C. Ten years of the fifth force. arXiv: hep-ph/9606249, and references therein.